

## Insight in shear banding under transient flow

J. P. Decruppe,<sup>1</sup> S. Lerouge,<sup>1</sup> and J. F. Berret<sup>2</sup>

<sup>1</sup>*Groupe Rhéophysique des Colloïdes, Laboratoire de Physique des Liquides et Interfaces, Université de Metz, 1 Boulevard François Arago, 57078 Metz, France*

<sup>2</sup>*Groupe de Dynamique des Phases Condensées, UMR 5581, Université de Montpellier II, Place Eugène Bataillon, 34095 Montpellier Cedex 5, France*

(Received 15 March 2000; published 22 January 2001)

The rheo-optical behavior of a viscoelastic solution of a surfactant subjected to transient shear flows is reported. A steplike shear rate is suddenly imposed and we record the transient physical characteristics of the liquid, i.e., the shear stress  $\sigma$ , the transmitted intensity  $I(t)$ , and the scattering pattern. At the inception of the flow the shear stress shows an important overshoot followed by damped oscillations which also appear in the intensity profile. Then a sigmoidal relaxation process brings the liquid in its final steady state. During this first phase, the diffusion pattern due to enhanced concentration fluctuations can also be observed. A fine anisotropic layer appears near the moving wall shortly after the inception of the flow, but its width starts to increase significantly well after the end of the relaxation process. When the laser beam travels through this band a diffraction pattern can be observed indicating that it is formed by small subbands, the characteristic width of which is in the order of 100  $\mu\text{m}$ .

DOI: 10.1103/PhysRevE.63.022501

PACS number(s): 83.50.-v

The flow of viscoelastic micellar solutions in a single laminar layer is known to become unstable when the shear stress  $\sigma$  reaches a critical value: the liquid contained in the gap of the shearing device separates in two bands which have different rheo-optical properties. This phenomenon, called ‘‘shear-banding,’’ predicted in the model of Spensley and Cates [1] based on the theoretical works of Doi and Edwards [2,3], has received much attention and many experimental studies have confirmed these predictions: rheology and small-angle neutron scattering (SANS) [4–9], flow birefringence (FB) [10–13], nuclear magnetic resonance (NMR) [14–17]. Many of these experiments are performed in a stationary state; the shear rate is slowly and gradually increased up to and beyond the critical shear rate where a highly anisotropic layer is formed, the proportion of which increases with  $\dot{\gamma}$ . For simplicity, in the following we shall call this layer the  $h$  band; it forms at first near the moving wall of the Couette cell, the rest of the gap is filled with the  $l$  band. This phenomenon has been well established by the above-mentioned techniques but is still not fully understood as concerns the emergence and the way the  $h$  band grows in width. In addition, the question of whether the shear banding flow is only a purely mechanical instability or involves a more subtle nucleation process as suggested by Berret and his co-workers [9] is not made clear by these stationary measurements. A deeper microscopic insight of the phenomenon, which occurs before the shear banding flow, is well established in the gap and can be reached through transient rheo-optical experiments, i.e., transient rheological, optical flow birefringence, and small-angle light scattering (SALS) experiments.

Berret *et al.* [9] have shown in the case of cetylpyridium chloride/sodium salicylate solutions (CPyCl/NaSal) solutions that the shear stress relaxation after a sudden inception of the flow happens on two different regimes, which extend over quite different time scales. The first one (corresponding to the overshoot and to the eventual damped oscillations) is

associated with a fast decrease of the shear stress over a time interval in the order of a few Maxwell times, while during the second domain,  $\sigma$  slowly decreases to reach its stationary value according to a sigmoidal profile,

$$\sigma \sim \exp \left[ - \left( \frac{t}{\tau_{NG(\dot{\gamma})}} \right)^\alpha \right].$$

This kind of stretched exponential decay has been explained in terms of a nucleation process followed by a one-dimensional growth of a nematic phase in the isotropic one.  $\tau_{NG(\dot{\gamma})}$  is the characteristic time for the nucleation and the one-dimensional (1D) growth processes. The analysis of the results of our optical experiments will not confirm this assumption: the nucleation process and the growth of the shear band seem to be two well distinct and independent phenomena [18].

The micellar solution chosen in this work is a solution of cetyltrimethylammonium bromide (CTAB) 0.3 M with a mineral salt, the sodium nitrate ( $\text{NaNO}_3$ ) at 1.79 M in water at  $T = 30^\circ\text{C}$ . This system is a good Maxwellian liquid with a single relaxation time ( $\tau_R \approx 0.18$  s), which shows a highly viscoelastic behavior and, as can also be expected, important nonlinear effects. For this high concentration, we can expect the micelles to form a highly entangled network. The aim of this paper is to compare the transient optical response of the micellar system to the time-dependent rheological studies in order to bring another insight in the shear banding phenomenon.

Figure 1 shows the variations of the stress versus the shear rate  $\dot{\gamma}$ . Three different curves can be seen; they are built in the following way: a typical transient flow curve [like the curve  $\sigma(t)$  in Fig. 2] shows an overshoot followed by a few oscillations and then a sigmoidal relaxation; three values of  $\sigma$  are of particular interest:  $\sigma_{os}$  ( $\Delta$ ) characterizes  $\sigma$  at the first overshoot,  $\sigma_M$  ( $\bullet$ ) is the extrapolated value of the stress after the first overshoot and just before the sigmoidal

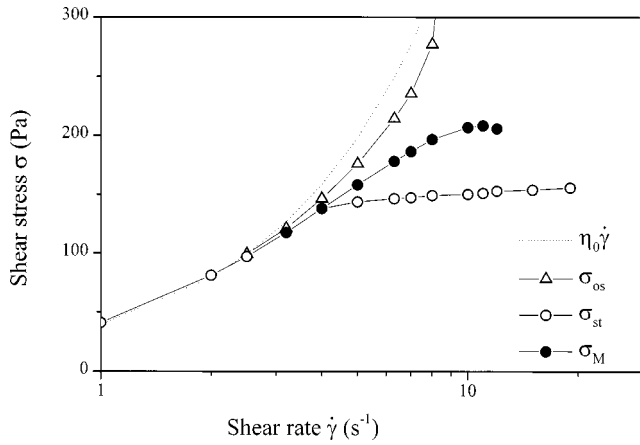


FIG. 1. Flow curves  $\sigma(\dot{\gamma})$  corresponding to different experimental values:  $\sigma_{os}$  is the value of  $\sigma$  at the overshoot,  $\sigma_{st}$  corresponds to the stationary value of the stress, and  $\sigma_M$  represents the extrapolated value of  $\sigma$  near 0 as described by Grand *et al.* [20].

relaxation, and finally  $\sigma_{st}$  (○) corresponds to the stationary value of the stress. The Newtonian variation ( $\sigma = \eta_0 \dot{\gamma}$ ) (dotted line) has been drawn for comparison. The reason for the choice of these particular values of the shear stress is described in great detail in another work [19]. It must be emphasized that the curve  $\sigma_M(\dot{\gamma})$  (●) looks very much like the curve  $\sigma(\dot{\gamma})$  we can get in strain controlled sweep experiments when the system is out of equilibrium. This procedure is similar to the one used by Grant and his co-workers [20]. The points forming the branch above the plateau shown by the curve  $\sigma_{st}$  (○) correspond to metastable states of the system and in the present work, we focus on a particular value ( $10 \text{ s}^{-1}$ ) which corresponds to the maximum of the curve  $\sigma_M(\dot{\gamma})$ . In a steady-state process during which  $\dot{\gamma}$  is slowly increased to  $10 \text{ s}^{-1}$ , the liquid would already have separated in two bands ( $\dot{\gamma}_c = 5 \text{ s}^{-1}$ ) which are not very stable (the interface fluctuates quite a lot for this particular solution), but nevertheless shows different optical properties. The physical device for these experiments is very simple: it is a stainless-steel Couette cell with the inner cylinder moving; the typical diameters are 47 and 50 mm. The temperature is kept constant to  $30^\circ$ . The moving wall is suddenly started and the maximum angular velocity is reached in a few milliseconds; the viscoelastic solution is thus subjected to a sharp step of shear rate and we record the evolution of the tangential shear stress  $\sigma(t)$  and of the transmitted light intensity; we also follow qualitatively the changes in the SALS patterns observed in both the planes  $(\vec{v}, \vec{\omega})$  and  $(\vec{v}, \vec{\nabla}_v)$ . As concerns the optical measurements, a narrow beam of laser light is sent through the medium in the direction of the vorticity. After traveling through 10 mm of solution, the beam hits a small pin diode which gives an electrical signal  $I(t)$  proportional to the quantity of energy received. Thus  $I(t)$  can be seen as a measurement of the turbidity of the solution. We have also checked that the solution did not show significant intrinsic dichroism which could be another way to explain the variation of  $I(t)$  under flow. We shall see that  $I(t)$  varies with time and that these variations result from light scattering which can be understood as form dichroism.

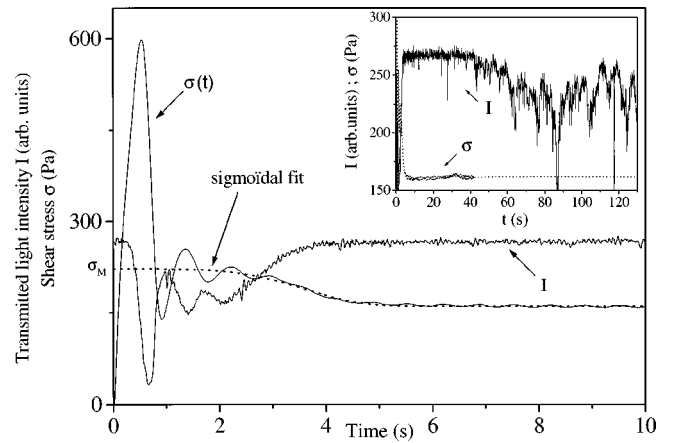


FIG. 2. Variations of the transmitted intensity  $I(t)$  (in arbitrary units) and of the shear stress versus time  $t$ . The small insertion shows  $I(t)$  on a larger time scale.

The second set of curves (Fig. 2) shows the variations of the shear stress  $\sigma$  and of the transmitted light intensity  $I$  (in arbitrary units) with the time  $t$ . The  $\sigma(t)$  curve is similar to the one described by Berret [7,19]; at the inception of the flow,  $\sigma$  increases sharply and very rapidly showing the typical overshoot of shear-thinning viscoelastic fluids. The peak reaches a maximum at  $t \approx 0.5 \text{ s}$  and  $\sigma = 600 \text{ Pa}$ , then the stress decreases very rapidly, oscillates a few times before the slow sigmoidal relaxation starts. Finally, after a few seconds (5–6 s) the steady state is reached and  $\sigma$  remains constant. The variations of  $\sigma$  should now be compared to those of  $I(t)$ . At time  $t=0$  and during the first few tenths of a second, when  $\sigma$  increases rapidly,  $I(t)$  is practically constant: the solution remains transparent; then it decreases sharply down to its minimum value which is reached when  $\sigma(t)$  is at its maximum. After this first period, the increase of  $I$  is associated with the sharp decrease of  $\sigma$  after the peak; it is remarkable to emphasize that the transmitted intensity also oscillates with  $t$  but is out of phase with  $\sigma(t)$ .

A direct observation of the gap with a microscope shows that the liquid becomes turbid: it takes the aspect of a milky solution which strongly scatters the light. Figure 3 presents a few SALS patterns chosen in the plane<sup>1</sup>  $(\vec{v}, \vec{\omega})$  and  $(\vec{v}, \vec{\nabla}_v)$  at various moments taken during the overshoot, the oscillations, and the sigmoidal relaxation of  $\sigma$ . Shortly after the inception of the flow, a typical butterfly pattern appears. This is particularly clear in the plane  $(\vec{v}, \vec{\omega})$  where a distinct figure can already be seen at 0.6 s while in the plane  $(\vec{v}, \vec{\nabla}_v)$  one has to wait for about 1 s before seeing the wings. This is only due to the weak sensitivity of our charge coupling device camera since a distinct pattern already exists at shorter times and can be directly observed on a translucent screen. The diffusion happens mainly after the peak of  $\sigma$ , during the fast decrease of  $\sigma$ , continues during the oscillations, diminishes, and finally vanishes during the sigmoidal relaxation. It is now commonly assumed that SALS results from spatio-

<sup>1</sup>Realized at the University of Montpellier.

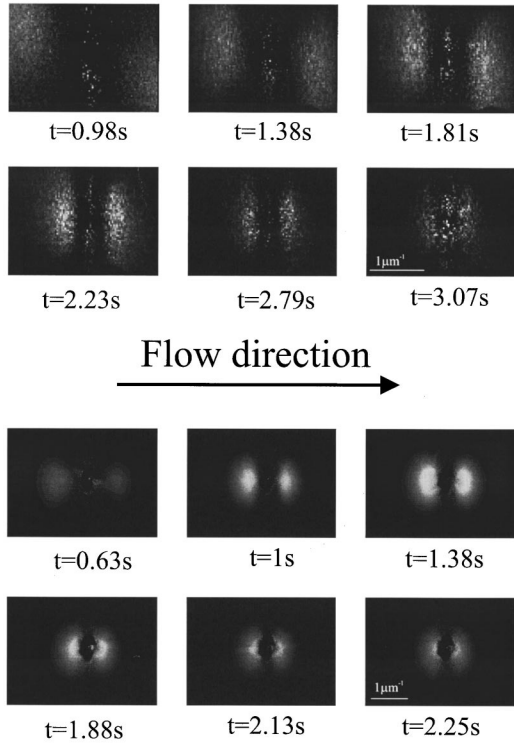


FIG. 3. A few diffusion patterns in the plane  $(\vec{v}, \nabla v)$  (upper half) and in the plane  $(\vec{\omega}, \vec{v})$  (lower half).

temporal fluctuations of the optical properties of the viscoelastic medium which are induced by concentration fluctuations. In that case, it can be shown [21] that the scattered intensity can be written as

$$I = ACS(\vec{q}),$$

with  $S(\vec{q}) = (1/C) \int \exp^{-\vec{q} \cdot \vec{x}} \langle \delta c(\theta) \delta c(\vec{x}) \rangle \vec{d}x$ , the structure factor, and  $\delta c(\vec{x})$  is a fluctuation at a point  $\vec{x}$ .

According to the Helfand-Fredrickson model [22], the concentration fluctuations are enhanced in the direction of the flow and suppressed in the direction of the gradient. Thus the oscillations of the tangential shear stress lead to periodical concentration fluctuations which induce periodical variations of  $I(t)$ . This assumption is confirmed by the SALS pattern which is nonmonotonic: a quite dim pattern corresponding to large  $\vec{q}$ 's appears right at the inception of the flow, disappears in half a second, before it reappears again around 0.63 s in the plane  $(\vec{v}, \vec{\omega})$  and 1 s in the plane  $(\vec{v}, \nabla v)$ . This evolution is particularly clear at lower shear rates ( $6-8 \text{ s}^{-1}$  not shown in this paper), where the frequency of this phenomenon is small compared to the frequency of the digitizing device. The evolution of  $\sigma(t)$  and  $I(t)$  are drawn on a longer time scale in the inset in Fig. 2. After the sigmoidal relaxation,  $\sigma(t)$  is constant and remains unchanged. However, this is not the case for  $I(t)$  which presents important fluctuations on and after 30–35 s. This can be explained by the set of photographs in Fig. 4 that shows a small portion of the gap in the plane  $(\vec{v}, \nabla v)$ . On each photograph, the lowest limit represents the inner moving cylin-

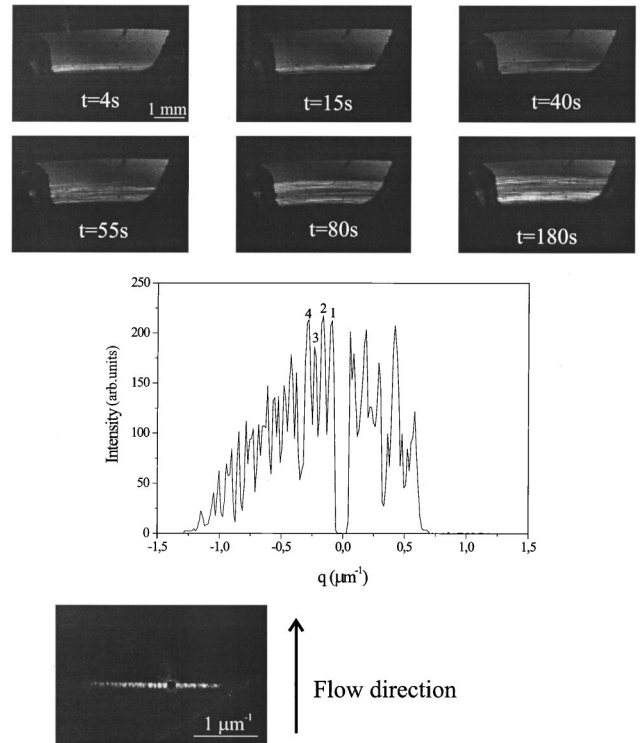


FIG. 4. The six photos show the gap of the Couette cell at various moments between 4 and 180 s. The figure  $I(q)$  represents the variation of the intensity in the diffusion pattern in a direction parallel to the bright streak. The maxima numbered 1–4 have been used to compute the width of the diffracting objects.

der. Shortly after the inception of the flow ( $t=4 \text{ s}$ ), a fine  $h$  band appears near the moving wall; at 5 s it is well established and its width remains approximately constant up to 25 s. At that time, the stress  $\sigma$  has reached its stationary value and the  $l$  band, which takes place in the rest of the gap, is transparent again as shown by the curve  $I(t)$ . Beyond 30 s, the proportion of the shear-induced phase significantly increases to finally spread over nearly two-thirds of the gap (see, for example, the last photograph of the set of six), and the laser beam that crosses the cell in the middle of the gap travels now through the  $h$  band. Thus the strong fluctuations of  $I(t)$  beyond 35 s are directly related to the increase of the width of the  $h$  band. If the transmitted light is collected on a screen, a “bright streak” [23–25] is observed in the direction of  $\nabla v$ . This pattern is quite unstable but we manage to take a few good pictures clearly showing a diffraction figure (see, for example, the photograph in Fig. 4, where distinct diffracted images of the beam can be seen especially in the left part of this pattern). This diffraction pattern looks very similar to the image we get when we illuminate a collection of narrow slits with different indexes of refraction. The variation of the diffracted intensity along the pattern has been digitized and from the curve  $I(q)$  (see Fig. 3), assuming a simple network, we can estimate the dimension of the diffracting object. We have used the peaks numbered 1 to 4 to perform this calculation and it turns out that  $d \approx 100 \mu\text{m}$ . So, we think that the pattern results from the diffraction of light

by a one-dimensional grid perpendicular to  $\vec{\nabla}v$  and with ‘‘slits’’ of roughly  $100\ \mu\text{m}$  width. This value is in quite good agreement with what we can observe in the gap with a microscope. In the  $h$  band, it is quite easy to see long threads parallel to the flow direction, the width of which is a fraction of a millimeter (see, for example in Fig. 4 the last photograph of the set of six). The laser beam is diffracted since the index of refraction of these threads is different from the index of the solution: this could result from the fact that the concentration of micelles is different in the threads and the  $h$  band appears as formed by two phases of different optical properties. When the laser beam travels through the  $l$  band, no diffraction pattern can be seen. Once the shearing flow is stopped the pattern slowly and gradually fades out, the outer peaks disappearing first, but it takes a long time for the first peaks on both sides of the central spot to completely vanish. The relaxation process is very slow, indicating that micelles

form longer structures aligned in a direction parallel to the flow in the  $h$  band.

In conclusion, these optical and rheological results clearly show that the nucleation process and the growing of the  $h$  band are two independent phenomena. Although a fine anisotropic layer is already present shortly after the overshoot, its width only increases when the steady-state regime is well established again. Shortly after the overshoot and for a short-time interval ( $\approx 2$  s), the light beam is strongly scattered and diffusion patterns are observed in both planes ( $\vec{v}, \vec{\nabla}v$ ) and ( $\vec{v}, \vec{\nabla}$ ). They reveal the existence of strong variations of the refraction index due to enhanced concentration fluctuations. The bright streak happens to be a diffraction pattern resulting from the scattering by small threadlike objects aligned in the direction of the flow. However, the highly anisotropic  $h$  band starts to grow well after the diffusion process and seems to be a completely independent process.

- 
- [1] N. A. Spenley, M. E. Cates, and T. C. B. MacLeish, *Phys. Rev. Lett.* **71**, 939 (1993).
- [2] M. Doi and S. F. Edwards, *J. Chem. Soc., Faraday Trans. 2* **75**, 918 (1978).
- [3] M. Doi and S. F. Edwards, *J. Chem. Soc., Faraday Trans. 2* **75**, 38 (1978).
- [4] J. F. Berret, D. C. Roux, G. Porte, and P. Lindner, *Europhys. Lett.* **25**, 521 (1994).
- [5] V. Schmitt, F. Lequeux, A. Pousse, and D. Roux, *Langmuir* **10**, 955 (1994).
- [6] E. Cappelare, J. F. Berret, J. P. Decruppe, R. Cressely, and P. Lindner, *Phys. Rev. E* **56**, 1869 (1997).
- [7] J. F. Berret, D. C. Roux, and P. Lindner, *Eur. Phys. J. B* **5**, 67 (1998).
- [8] H. Rehage and H. Hoffmann, *J. Phys. Chem.* **92**, 4712 (1988); *Mol. Phys.* **74**, 933 (1991).
- [9] J. F. Berret, D. C. Roux, and G. Porte, *J. Phys. II* **4**, 1261 (1994).
- [10] J. P. Decruppe, R. Cressely, R. Makhoulfi, and E. Cappelare, *Colloid Polym. Sci.* **273**, 346 (1995).
- [11] R. Makhoulfi, J. P. Decruppe, A. Ait-Ali, and R. Cressely, *Europhys. Lett.* **32**, 253 (1995).
- [12] J. P. Decruppe, E. Cappelare, and R. Cressely, *J. Phys. II* **7**, 257 (1997).
- [13] J. F. Berret, G. Porte, and J. P. Decruppe, *Phys. Rev. E* **55**, 1 (1997).
- [14] R. W. Mair and P. T. Callaghan, *Europhys. Lett.* **65**, 241 (1996).
- [15] P. T. Callaghan, M. E. Cates, C. J. Rofe, and J. B. A. F. Smeulders, *J. Phys. II* **6**, 375 (1996).
- [16] R. W. Mair and P. T. Callaghan, *Europhys. Lett.* **36**, 9 (1996).
- [17] M. M. Britton and P. T. Callaghan, *Phys. Rev. Lett.* **78**, 26 (1997).
- [18] S. Lerouge, J. P. Decruppe, and J. F. Berret (unpublished).
- [19] J. F. Berret, *Langmuir* **13**, 2227 (1997).
- [20] C. Grand, J. Arrault, and M. E. Cates, *J. Phys. II* **7**, 1071 (1997).
- [21] G. G. Fuller, *Optical Rheometry of Complex Fluids* (Oxford University Press, Oxford, 1995).
- [22] E. Helfand and G. H. Fredrickson, *Phys. Rev. Lett.* **62**, 2468 (1989).
- [23] E. K. Wheeler, I. Pilar, and G. G. Fuller, *Rheol. Acta* **35**, 139 (1996).
- [24] S. Lerouge, J. P. Decruppe, and C. Humbert, *Phys. Rev. Lett.* **81**, 5457 (1998).
- [25] I. A. Kadoma and J. W. van Egmond, *Phys. Rev. Lett.* **76**, 4432 (1996).